CMS Physics Analysis Summary

Contact: cms-pag-conveners-exotica@cern.ch 2017/03/22

Search for evidence of Type-III seesaw mechanism in multilepton final states in pp collisions at $\sqrt{s} = 13$ TeV

The CMS Collaboration

Abstract

A search for a type-III seesaw signal in events with three or more electrons or muons is presented. The data sample corresponds to 35.9 fb^{-1} of integrated luminosity in pp collisions at $\sqrt{s} = 13$ TeV collected by the CMS experiment at the LHC in 2016. The signal is sought after in final states with at least three leptons, and has diverse kinematic properties. The primary selection is based on the number of leptons and the invariant mass of opposite-sign lepton pairs, and helps discriminate the signal against the standard model background. The final optimization for the type-III seesaw signal is based on the sum of leptonic transverse momenta and missing transverse energy, as well as the transverse mass. The observations are consistent with expectations from standard model processes. The results are used to exclude heavy fermions of the type-III seesaw model with masses below 850 GeV for the lepton-flavor democratic scenario.

The discovery of neutrino oscillations indicated that neutrinos are massive [1] and gave strong motivation for physics beyond the standard model (SM). Several extensions of the SM to address neutrino masses have been proposed so far, among which the seesaw mechanism is an appealing possibility [2–12]. The seesaw mechanism introduces new heavy particles coupling to leptons and to the Higgs doublets, and accounts for the expected smallness of neutrino masses. Within the type-III seesaw model [13], the neutrino is considered a Majorana particle whose mass arises via the mediation of new massive fermions. These massive fermions are an *SU(2)* triplet of heavy Dirac charged leptons $\Sigma^{\pm}$, and a heavy Majorana neutral lepton Σ^0. In proton-proton collisions, these massive fermions may be pair-produced through electroweak interactions in both charged-charged and charged-neutral pairs. We conduct a search for these new massive fermions by examining the final state with at least three leptons (electrons or muons) [14, 15]. This final state arises due to the following decays $\Sigma^{\pm} \to \mathrm{W}^{\pm}\nu$, $\Sigma^{\pm} \to Z\ell^{\pm}$, $\Sigma^{\pm} \to H\ell^{\pm}$, $\Sigma^0 \to \mathrm{W}^{\pm}\ell^{\mp}$, $\Sigma^0 \to Z\nu$, and $\Sigma^0 \to H\nu$, where $\ell = e, \mu$ or τ. Decays of $\Sigma^0\Sigma^{\pm}$ and $\Sigma^+\Sigma^-$ pairs result in 27 distinct processes and can naturally lead to multilepton final states if several W or Z bosons are involved, either directly or via a Higgs boson decay [16]. A complete decay chain example would be $\Sigma^{\pm}\Sigma^0 \to \mathrm{W}^{\pm}\nu\mathrm{W}^{\pm}\ell^{\mp} \to \ell^{\pm}\nu\nu\ell^{\pm}\nu\ell^{\mp}$.

We simulate all 27 distinct signal production and decay combinations of the seesaw signal using model files provided by the authors of Ref. [16] as input to MADGRAPH 5 aMC@NLO [17]. In this implementation, the $\Sigma^{\pm}$ and Σ^0 are degenerate in mass, their decays are prompt, and the Σ decays are democratic in e, μ, and τ lepton flavors (flavor-democratic scenario). This is done by taking the mixing angles to be $V_e = V_\mu = V_\tau = 10^{-6}$. This has no direct consequences on the fermion production cross section, but affects the branching ratios. The branching fraction of a heavy fermion to a lepton of flavor ℓ is proportional to $v_{\ell N} = V_\ell/(|V_e|^2 + |V_\mu|^2 + |V_\tau|^2)^{1/2}$. Therefore the flavor-democratic scenario gives $v_{\ell N} = 1/\sqrt{3}$.

Prior searches from CMS have been conducted using the 7 TeV data [18] and the 8 TeV data [19]. Using 8 TeV data, ATLAS excluded m_Σ below 335 GeV probing a similar scenario, but assuming that the Σ's decay only to electrons and muons [20]. The strongest constraints in the flavor-democratic scenario are from a CMS search using the 13 TeV data collected in 2015, and exclude m_Σ below 440 GeV [21].

We pursue a broad search in final states with at least three isolated prompt leptons using 35.9 fb^{-1} of pp collision data collected in 2016 at $\sqrt{s} = 13$ TeV. The notable backgrounds can be classified as irreducible backgrounds from the production and decay of dibosons (WZ and ZZ production), and reducible backgrounds from leptonic Z or $\mathrm{t\bar{t}}$ production and decay accompanied by leptons from heavy-flavor quark decays, or from misidentification of jets as leptons. In addition, small backgrounds also arise from SM processes such as $\mathrm{t\bar{t}}W$, $\mathrm{t\bar{t}}Z$, triboson, and Higgs production.

The CMS detector [22] has cylindrical symmetry around the pp beam axis with tracking and muon detectors covering the pseudorapidity range $|\eta| < 2.4$. The tracking system measures the trajectory and momentum of charged particles and consists of multilayered silicon pixel and strip detectors in a 3.8 T solenoidal magnetic field. Particle energies are measured with concentric electromagnetic and hadron calorimeters, which cover $|\eta| < 3.0$ and $|\eta| < 5.0$, respectively. Muon detectors consisting of wire chambers are embedded in the steel return yoke outside the solenoid. The trigger thresholds of a two-level trigger system are tuned to accept a few hundred data events per second from the pp interactions.

The data for this search are collected using several dilepton triggers. The double electron trigger requires two electrons with a p_T threshold of 23 (12) GeV on the leading (subleading) electron. The double muon trigger requires two muons with a p_T threshold of 17 (8) GeV on the

leading (subleading) muon. We use two muon/electron cross trigger combinations, one of which require a 23 GeV muon and an 8 GeV electron, while the other requires an 23 GeV electron and a 8 GeV muon.

The signal is generated using MADGRAPH 5 aMC@NLO v5.2.2 [23] at LO precision using the NNPDF30_lo_as_0130_nf_4 [24] parton density function (PDF). The signal cross section is calculated to NLO + NLL accuracy, as for generic *SU(2)* fermion triplets [25, 26], and is used to estimate signal yields. The diboson background samples (WZ, ZZ) are generated using POWHEG V2 [27, 28]. The triboson backgrounds are generated using MADGRAPH 5 aMC@NLO v5.2.2 whereas backgrounds from Higgs production are generated using POWHEG V2 and JHU Generator v6.2.8 [29–32]. Bosonic decays, along with parton showering, fragmentation and hadronization for all samples are performed using PYTHIA 8.212 [33, 34]. For systematic studies, we also use simulation samples for Z and $\mathrm{t\bar{t}}$ production generated using MADGRAPH 5 aMC@NLO v5.2.2.

The response of the CMS detector is simulated using dedicated software based on the GEANT4 toolkit [35]. All simulation samples are corrected for mismodeling of additional interactions in the same bunch crossing (pile-up). In addition, we apply weights to all simulated events to account for differences in trigger and lepton identification efficiencies between data and simulation.

Events that pass the trigger are required to satisfy additional offline selections. Electrons and muons with $p_{\mathrm{T}} > 10\,\mathrm{GeV}$ and $|\eta| < 2.5$ ($|\eta| < 2.4$ for muons) are reconstructed using the particle-flow (PF) algorithm which utilizes measured quantities from the tracker, calorimeter, and muon system [36]. Candidate electrons and muons must have tracks satisfying quality requirements and spatially match with the energy deposits in the ECAL and the tracks in the muon detectors, respectively.

The backgrounds to this analysis consist of prompt leptons arising from boson decay, as well as non-prompt leptons. Non-prompt leptons include leptons arising from heavy-flavor quark decays, or from leptons occurring inside or near jets, as well as misidentified leptons from hadrons that punch through into the muon system, or from hadronic showers with large electromagnetic fractions. Henceforth we collectively refer to all non-prompt leptons as misidentified leptons.

An isolation requirement that compares the p_{T} of a lepton to the sum p_{T} of particles in its immediate neighborhood, strongly reduces the backgrounds from misidentified leptons. We consider relative isolation, defined as the scalar sum of the transverse momenta of photon and charged and neutral hadron candidates reconstructed by the PF algorithm within a cone of given size around the lepton candidate normalized to the lepton candidate p_{T}, for both muons and electrons. This relative isolation is required to be less than 25% within a cone of size $R = 0.4$ for muons, and less than 7% and 8% within a cone of size $R = 0.3$ for electrons whose energy deposits are reconstructed in ECAL barrel ($|\eta| < 1.479$) and in ECAL endcap ($|\eta| > 1.479$), respectively. All isolation quantities are corrected for contributions of particles originating from pileup vertices.

We further reduce the misidentified lepton backgrounds by requirements on the longitudinal (d_z) and transverse (d_{xy}) impact parameters of leptons with respect to the primary interaction point in the event. We require that the muons satisfy $|d_z| < 0.1\,\mathrm{cm}$, and $|d_{xy}| < 0.05\,\mathrm{cm}$. For electrons, we require $|d_z| < 0.1\,\mathrm{cm}$, $|d_{xy}| < 0.05\,\mathrm{cm}$ in the ECAL barrel, and $|d_z| < 0.2\,\mathrm{cm}$, $|d_{xy}| < 0.1\,\mathrm{cm}$ in the ECAL endcap.

Jets are reconstructed from the charged and neutral hadron, muon, electron, and photon PF

Table 1: The signal regions used in this search are summarized in terms of the number of leptons, the presence of an OSSF pair, and the kinematic variable used for discrimination. Each selection described here is further divided into eight bins in the kinematic variable, giving a total of 48 statistically independent signal regions. Additional criteria used to ensure that signal regions are non-overlapping with control regions are also stated.

N_{leptons}	OSSF	Kinematic Variable	CR-veto
3	on-Z	M_{T}	$E_{\text{T}}^{\text{miss}} > 100\,\text{GeV}$
	above-Z	$L_{\text{T}} + E_{\text{T}}^{\text{miss}}$	-
	below-Z	$L_{\text{T}} + E_{\text{T}}^{\text{miss}}$	$E_{\text{T}}^{\text{miss}} > 50\,\text{GeV}$
	none	$L_{\text{T}} + E_{\text{T}}^{\text{miss}}$	-
≥ 4	1 pair	$L_{\text{T}} + E_{\text{T}}^{\text{miss}}$	-
	2 pairs	$L_{\text{T}} + E_{\text{T}}^{\text{miss}}$	$E_{\text{T}}^{\text{miss}} > 50\,\text{GeV}$ if on-Z

candidates using the anti-k_t algorithm with distance parameter of $R = 0.4$ [37]. Jets are required to have $p_{\text{T}} \geq 30\,\text{GeV}$ and $|\eta| \leq 3.0$ and satisfy quality criteria to remove contributions from particles arising from other interactions in the same bunch crossing.

The missing transverse momentum is calculated as the negative vectorial sum of the transverse momenta of all the PF candidates. The missing transverse energy $E_{\text{T}}^{\text{miss}}$ is defined as the magnitude of this vector. Jet energy corrections are applied to all jets and also propagated to the calculation of $E_{\text{T}}^{\text{miss}}$ [38].

For the three leading leptons, we apply offline thresholds of 25, 15, 10 GeV. Additional leptons are also considered only if they satisfy $p_{\text{T}} > 10\,\text{GeV}$. We find that with these thresholds, the trigger efficiency of trilepton events is close to 100%. Events with an opposite-sign same-flavor (OSSF) lepton pair with mass below 12 GeV are vetoed to reduce background from low-mass resonances. We reject trilepton events with an OSSF pair with mass below 81 GeV, when the trilepton mass is within a Z-mass window ($91 \pm 10\,\text{GeV}$). This reduces background from asymmetric photon conversions in $Z \to \ell\ell^* \to \ell\ell\gamma$, where the photon converts into two additional leptons, one of which is lost.

We classify the selected multilepton events into statistically independent search channels using the number of leptons, lepton flavor and charge combinations, and other kinematic quantities. We count the number of OSSF pairs made using each lepton only once. For example, $\mu^+\mu^-\mu^-$ is OSSF1, while $\mu^+\mu^-e^-e^+$ is OSSF2. We further classify events in three categories as on-Z, below-Z, and above-Z, based on the presence of at least one OSSF pair with mass in the Z-mass window, below 81 GeV, or above 101 GeV, respectively. In cases of ambiguity (such as $\mu^+\mu^-\mu^-$), the OSSF pair with mass closest to that of the Z boson takes precedence.

We construct the scalar sum of all lepton p_{T}, labeled as L_{T}. As the main discriminating variable, we use $L_{\text{T}} + E_{\text{T}}^{\text{miss}}$. This choice allows us to maintain sensitivity to decay modes such as $\Sigma^{\pm} \to \ell^{\pm}Z \to \ell^{\pm}\ell^{\pm}\ell^{\mp}$ with large lepton momenta, as well as $\Sigma^0 \to H\nu \to WW\nu$, where lepton p_{T} s are lower but the neutrinos contribute to $E_{\text{T}}^{\text{miss}}$. For events which are OSSF1, on-Z, we observe an improved sensitivity by considering the transverse mass, $M_{\text{T}} = (2E_{\text{T}}^{\text{miss}} p_T^{\ell}(1 - cos\measuredangle(\vec{E}_{\text{T}}^{\text{miss}}, \vec{p}_T^{\,\ell})))^{1/2}$ using the lepton that is not part of the OSSF pair. The optimum requirement on $L_{\text{T}} + E_{\text{T}}^{\text{miss}}$, or M_{T} depends on the mass of the heavy fermions. To maintain high sensitivity across the expected mass range, we categorize the data in eight bins of $L_{\text{T}} + E_{\text{T}}^{\text{miss}}$, or M_{T}. We use bins of width 150 (100) GeV for $L_{\text{T}} + E_{\text{T}}^{\text{miss}}$ (M_{T}), and in each case the highest bin includes overflows.

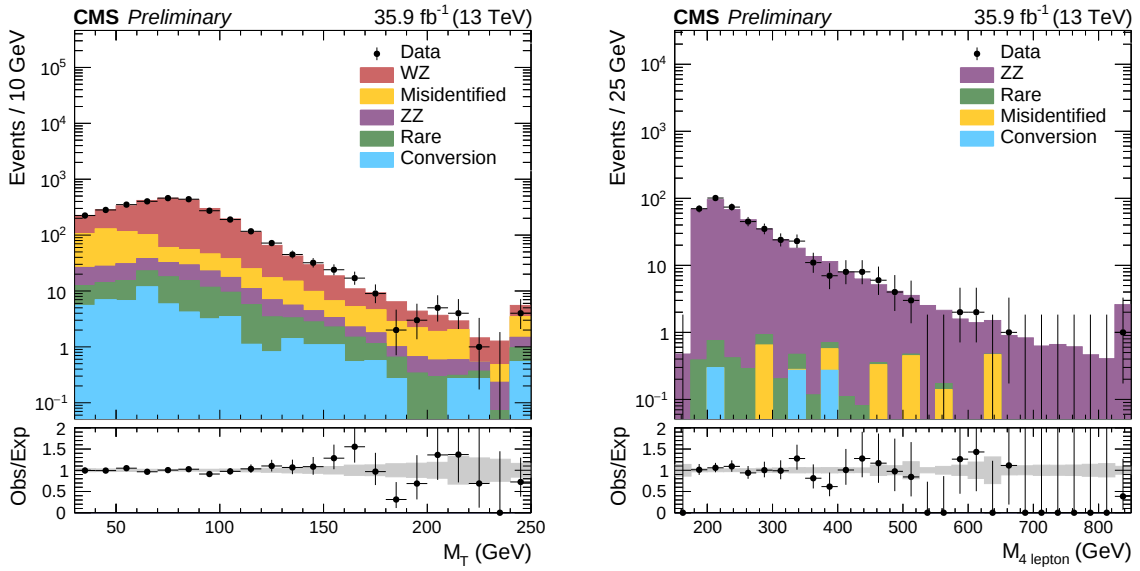

Figure 1: The M_{T} distribution in a WZ enriched selection of events with three leptons and one OSSF pair with mass on-Z, $50 < E_{\mathrm{T}}^{\mathrm{miss}} < 100$ GeV and $M_{\mathrm{T}} > 30$ GeV (left), and the four-lepton invariant mass distribution in a ZZ enriched selection of events with four leptons and two OSSF pairs both of which are on-Z and $E_{\mathrm{T}}^{\mathrm{miss}} < 50$ GeV (right). The total SM background is shown as a stack of all contributing processes, and the gray band in the lower panel represents the statistical uncertainty on the expected background.

As a result, we have eight independent signal regions in each of the following five $L_{\mathrm{T}} + E_{\mathrm{T}}^{\mathrm{miss}}$ distributions for events with (i) three leptons, OSSF0; (ii) three leptons, OSSF1, below-Z; (iii) three leptons, OSSF1, above-Z; (iv) four or more leptons, OSSF1; and (v) four or more leptons, OSSF2. In addition, we consider eight independent signal regions for a selection with three leptons, OSSF1, on-Z with kinematic binning in M_{T}. The total 48 orthogonal signal regions are summarized in Table 1.

The irreducible backgrounds are estimated using dedicated simulation samples, and are dominated by the WZ and ZZ processes. These processes are normalized to data using dedicated control selections. For WZ, we select events with exactly three leptons, with OSSF1 on-Z, $50 < E_{\mathrm{T}}^{\mathrm{miss}} < 100\,\mathrm{GeV}$, and $M_{\mathrm{T}} > 30\,\mathrm{GeV}$. The ratio of WZ prediction to data (after corrections of non-WZ events) is found to be 1.15 ± 0.08, where the uncertainty includes both statistical and systematic contributions. Similarly, for ZZ, we select events with exactly four leptons, $E_{\mathrm{T}}^{\mathrm{miss}} < 50\,\mathrm{GeV}$, with OSSF2 and both pairs satisfying on-Z, and the ratio of ZZ prediction to data is found to be 1.25 ± 0.06. These normalization factors are then used for the WZ and ZZ background estimates. Figure 1 shows the M_{T} distribution in the WZ enriched selection, and the four lepton invariant mass distribution in the ZZ enriched selection. We also use these control selections to test our modeling of kinematic distributions of interest such as $L_{\mathrm{T}} + E_{\mathrm{T}}^{\mathrm{miss}}$ and M_{T}. The other irreducible backgrounds from triboson, $\mathrm{t\bar{t}}W$, $\mathrm{t\bar{t}}Z$, and Higgs processes are estimated from simulation using the theoretically calculated cross sections, and are referred to as "rare" backgrounds in this note.

The backgrounds from misidentified leptons arise from processes such as Z+jets, and $\mathrm{t\bar{t}}$. These are estimated using a 3-dimensional implementation of a matrix method [39]. The matrix method is a data-driven method that assumes that the probabilities of prompt and misidentified leptons to pass a tight lepton selection, given that they pass a loose lepton selection, are universal. These probabilities, called prompt and misidentification rates, are functions of

lepton- and event-dependent parameters. We measure these rates using dedicated selections; a dilepton selection for prompt rates, and a trilepton signal depleted selection (OSSF1 on-Z, $E_{\mathrm{T}}^{\mathrm{miss}} < 50\,\mathrm{GeV}$) for misidentification rates. The rates are parametrized as a function of lepton p_{T}, η, and the number of particles around the lepton. The rates measured in data are dominated by Z+jets events, and are corrected using simulation to an average of Z+jets and $\mathrm{t\bar{t}}$+jets events.

A residual background from photon conversions remains, which is also estimated using a data-driven method. This background, referred to as "conversion" background, is dominated by final-state photon radiation from an existing lepton, where the photon then converts asymmetrically to two additional leptons, only one of which is reconstructed in the detector. To estimate this background, we obtain a rate that relates events with three leptons to those with two leptons and a photon. We consider trilepton events where the trilepton mass is on-Z, but the dilepton mass is below-Z. These events are compared with dilepton+photon events where the dilepton invariant mass is below-Z, but the combined invariant mass of the two leptons and the photon is on-Z. To ensure that we select photons radiated from leptons, we veto photons that are far away from a lepton and are close to a jet. Additional criteria based on photon E_{T} and lepton p_{T} are used to further reject photons that are not suitable for modeling conversions. This rate is then used to scale the observed number of dilepton+photon events in a given signal region to estimate the background from photon conversions.

The WZ and ZZ backgrounds have systematic uncertainties of 7% and 5%, respectively, arising from the normalization factor measurements. The rare backgrounds have an uncertainty of 50% on the theory cross section, along with the uncertainty of 2.5% due to luminosity measurement.

The final misidentified background estimate is assigned an uncertainty of 30%. This is dominated by differences in the rates in Z+jets and $\mathrm{t\bar{t}}$+jets events, and is derived by varying the prompt and misidentification rates up and down for each lepton flavor within their respective uncertainties. The photon conversion background also has a 30% uncertainty which primarily arises due to contamination by non-conversion backgrounds in the rate measurement region.

A minor source of systematic uncertainty is due to the corrections applied to the simulated background events to account for differences with respect to data events in lepton identification and isolation efficiencies, dilepton trigger efficiencies, as well as electron, muon and jet energy or momentum scale and resolution measurements. The uncertainties due to these corrections are considered separately, and result in a 1-10% variation of the simulation based background yields across all signal regions.

The uncertainties on signal acceptance due to the PDF uncertainties are estimated by utilizing the replica weights of the NNPDF30_lo_as_0130_nf_4 PDF set, and found to be less than 3% in all signal bins. The signal yields also have uncertainties due to luminosity measurement as well as the simulation correction based contributions mentioned in the previous paragraph.

We observe no statistically significant excess in the various signal regions that we probe. Figures 2 and 3 show the results in all 48 signal regions. Assuming a flavor-democratic scenario, we calculate a 95% confidence level upper limit on the cross section sum for the production of heavy fermion pairs ($\Sigma^0\Sigma^+$, $\Sigma^0\Sigma^-$, or $\Sigma^+\Sigma^-$), using the the CLs method [40–43]. Based on the observed cross section limits, we rule out the production of heavy fermion pairs for masses less than 850 GeV (expected 790 GeV), as presented in Figure 4. The signal cross section has an uncertainty of approximately 5-15% due to scale and choice of PDF in the mass range we consider and this uncertainty is shown in the figure.

In summary, we performed a search for type-III seesaw heavy fermions in multilepton final states using $35.9\,\mathrm{fb}^{-1}$ of proton-proton collision data at $\sqrt{s} = 13\,\mathrm{TeV}$, collected using the CMS

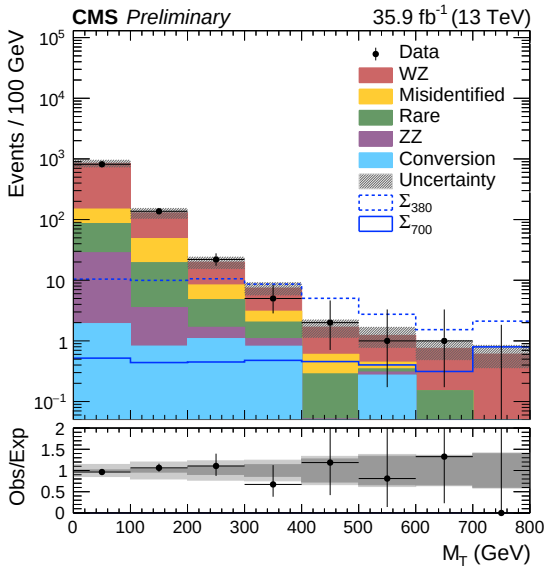

(a) M_{T}, L3OnZ

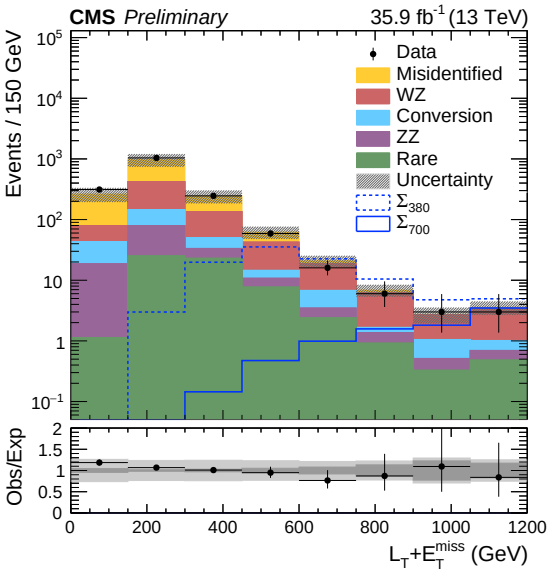

(b) $L_{\mathrm{T}} + E_{\mathrm{T}}^{\mathrm{miss}}$, L3AboveZ

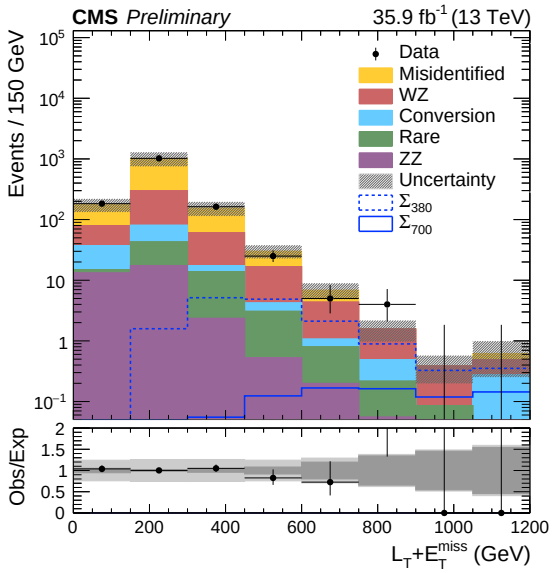

(c) $L_{\mathrm{T}} + E_{\mathrm{T}}^{\mathrm{miss}}$, L3BelowZ

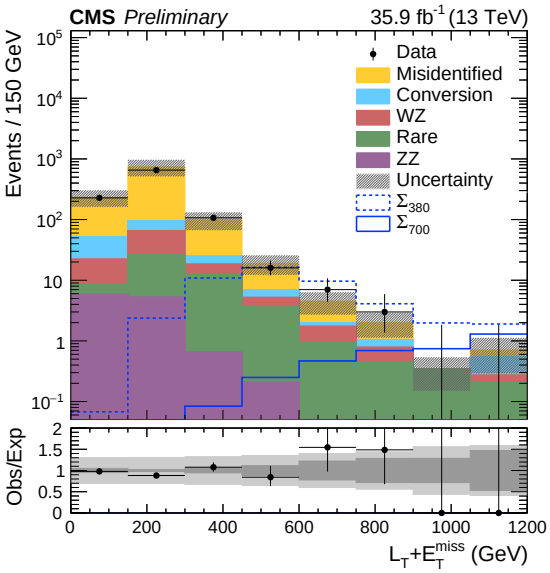

(d) $L_{\mathrm{T}} + E_{\mathrm{T}}^{\mathrm{miss}}$, L3OSSF0

Figure 2: The M_{T} distribution for events with three leptons and one OSSF pair, with mass on-Z and $E_{\mathrm{T}}^{\mathrm{miss}} > 100\,\mathrm{GeV}$ (top left), the $L_{\mathrm{T}} + E_{\mathrm{T}}^{\mathrm{miss}}$ distribution for events with three leptons and one OSSF pair with mass above-Z (top right), the $L_{\mathrm{T}} + E_{\mathrm{T}}^{\mathrm{miss}}$ distribution for events with three leptons and one OSSF pair, with mass below-Z and $E_{\mathrm{T}}^{\mathrm{miss}} > 50\,\mathrm{GeV}$ (bottom left) and with three leptons and no OSSF pairs (below right). The total SM background is shown as a stack of all contributing processes. The predictions for signal models with $m_{\Sigma} = 700\,\mathrm{GeV}$ (solid line) and $m_{\Sigma} = 380\,\mathrm{GeV}$ (dashed line) (sum of all production and decay modes) are also shown. The hatched gray band in the upper panel, and the dark and light gray bands in the lower panel represent the total, statistical, and systematic uncertainties on the expected background, respectively.

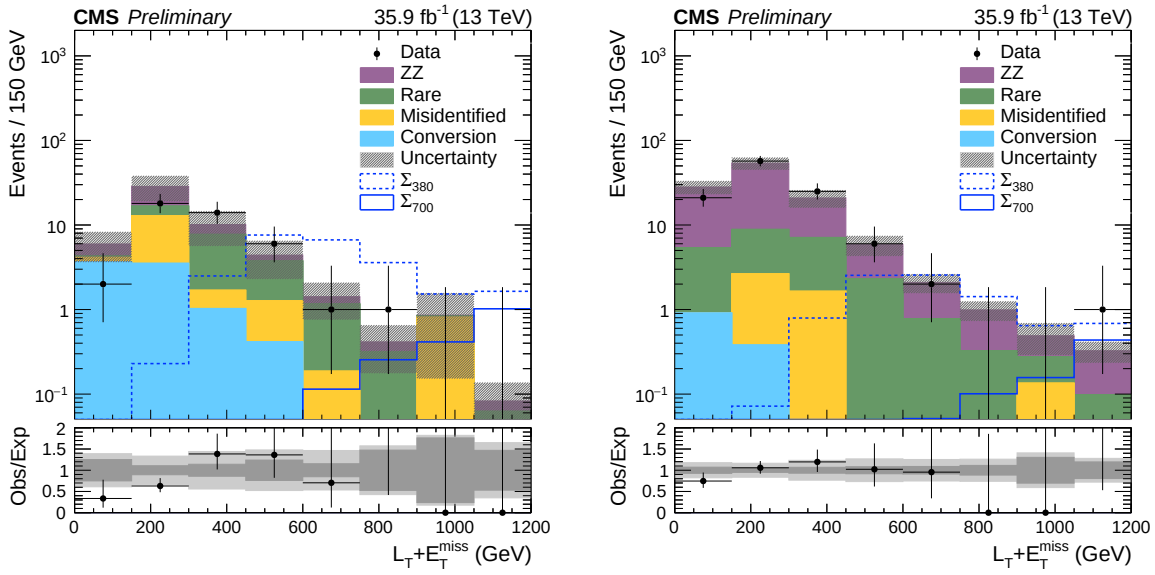

Figure 3: The $L_{\mathrm{T}} + E_{\mathrm{T}}^{\mathrm{miss}}$ distribution for events with four or more leptons and one OSSF pair (left), and with four or more leptons and at least two OSSF pairs (right). The total SM background is shown as a stack of all contributing processes. The predictions for signal models with $m_{\Sigma} = 700\,\mathrm{GeV}$ (solid line) and $m_{\Sigma} = 380\,\mathrm{GeV}$ (dashed line) (sum of all production and decay modes) are also shown. The hatched gray band in the upper panel, and the dark and light gray bands in the lower panel represent the total, statistical, and systematic uncertainties on the expected background, respectively.

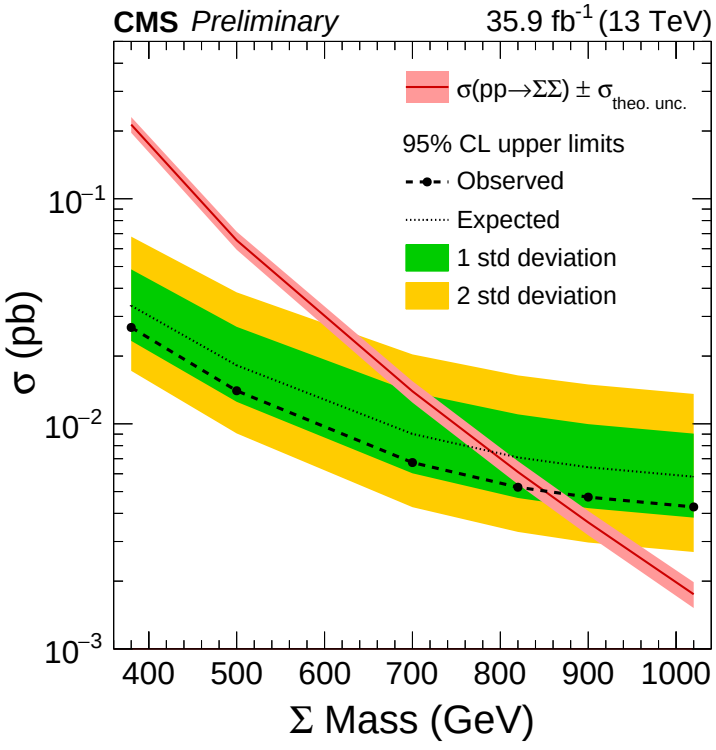

Figure 4: The 95% confidence level upper limits on the cross section sum for production of heavy fermion pairs ($\Sigma^0\Sigma^+$, $\Sigma^0\Sigma^-$, or $\Sigma^+\Sigma^-$). In the flavor-democratic scenario, we rule out heavy fermion pair production for masses below 850 GeV (expected 790 GeV).

detector. We observe no significant discrepancies between the background prediction and the data. Assuming degenerate heavy fermion masses m_Σ, we exclude previously unexplored regions of the signal model with heavy fermion particle with a mass limit for the lepton-flavor democratic scenario of 850 GeV at 95% confidence level.

References

[1] F. Capozzi et al., "Status of three-neutrino oscillation parameters, circa 2013", *Phys. Rev. D* **89** (2014) 093018, arXiv:1312.2878.

[2] P. Minkowski, "$\mu \to e\gamma$ at a rate of one out of 10^9 muon decays?", *Phys. Lett. B* **67** (1977) 421, doi:10.1016/0370-2693(77)90435-X.

[3] M. Gell-Mann, P. Ramond, and R. Slansky, "Neutrino Mass in seesaw type I", *Sanibel Talk* **CALT-68-709** (1979).

[4] T. Yanagida, "Neutrino Mass in seesaw type I", *Proc. of the Workshop on Unified Theory and Baryon Number of the Universe* **64** (1979) 1103.

[5] R. Mohapatra, N. Rabindra, and G. Senjanovic, "Neutrino Mass and Spontaneous Parity Violation", *Phys. Rev. Lett.* **44** (1980) 912, doi:10.1103/PhysRevLett.44.912.

[6] M. Magg and C. Wetterich, "Neutrino Mass Problem and Gauge Hierarchy", *Phys. Rev. B* **94** (1980) 61, doi:10.1016/0370-2693(80)90825-4.

[7] R. Mohapatra and G. Senjanovic, "Neutrino Masses and Mixings in Gauge Models with Spontaneous Parity Violation", *Phys. Rev. D* **23** (1981) 165, doi:10.1103/PhysRevD.23.165.

[8] E. Ma and U. Sarkar, "Neutrino masses and leptogenesis with heavy Higgs triplets", *Phys. Rev. Lett.* **80** (1998) 5716–5719, doi:10.1103/PhysRevLett.80.5716, arXiv:hep-ph/9802445.

[9] R. Foot, H. Lew, X. He, and G. Joshi, "See-saw neutrino masses induced by a triplet of leptons", *Z. Phys. C* **44** (1989) doi:10.1007/BF01415558.

[10] R. N. Mohapatra, "Mechanism for understanding small neutrino mass in superstring theories", *Phys. Rev. Lett.* **56** (Feb, 1986) 561–563, doi:10.1103/PhysRevLett.56.561.

[11] R. N. Mohapatra and J. W. F. Valle, "Neutrino mass and baryon-number nonconservation in superstring models", *Phys. Rev. D* **34** (Sep, 1986) 1642–1645, doi:10.1103/PhysRevD.34.1642.

[12] W.-Y. Keung and G. Senjanović, "Majorana Neutrinos and the Production of the Right-Handed Charged Gauge Boson", *Phys. Rev. Lett.* **50** (May, 1983) 1427, doi:10.1103/PhysRevLett.50.1427.

[13] R. Foot, H. Lew, X. He, and G. Joshi, "See-saw neutrino masses induced by a triplet of leptons", *Z. Phys. C* **44** (1989) doi:10.1007/BF01415558.

[14] F. del Aguila and J. A. Aguilar-Saavedra, "Distinguishing seesaw models at LHC with multi-lepton signals", *Nucl. Phys.* **B813** (2009) 22–90, doi:10.1016/j.nuclphysb.2008.12.029, arXiv:0808.2468.

[15] F. del Aguila, J. A. Aguilar-Saavedra, and J. de Blas, "Trilepton signals: the golden channel for seesaw searches at LHC", *Acta Phys. Polon.* **B40** (2009) 2901–2911, arXiv:0910.2720.

[16] C. Biggio and F. Bonnet, "Implementation of the type III seesaw model in FeynRules/MadGraph and prospects for discovery with early LHC data", *Eur. Phys.J. C* **72** (2012) 1899, doi:10.1140/epjc/s10052-012-1899-z, arXiv:1107.3463v3.

[17] J. Alwall et al., "The automated computation of tree-level and next-to-leading order differential cross sections, and their matching to parton shower simulations", *JHEP* **07** (2014) 079, doi:10.1007/JHEP07(2014)079, arXiv:1405.0301.

[18] CMS Collaboration, "Search for heavy lepton partners of neutrinos in proton-proton collisions in the context of the type III seesaw mechanism", *Phys. Lett.* **B718** (2012) 348, doi:10.1016/j.physletb.2012.10.070, arXiv:1210.1797.

[19] CMS Collaboration, "Search for heavy lepton partners of neutrinos in pp collisions at 8 TeV, in the context of type III seesaw mechanism", Technical Report CMS-PAS-EXO-14-001, CERN, Geneva, 2015.

[20] ATLAS Collaboration, "Search for type-III Seesaw heavy leptons in pp collisions at 8 TeV with the ATLAS Detector", *Phys. Lett. D* **92** (2015) 032001, doi:10.1103/PhysRevD.92.032001, arXiv:1506.01839.

[21] CMS Collaboration, "Search for Type-III Seesaw Heavy Fermions with Multilepton Final States using 2.3/fb of 13 TeV proton-proton Collision Data", Technical Report CMS-PAS-EXO-16-002, CERN, Geneva, 2016.

[22] CMS Collaboration, "The CMS experiment at the CERN LHC", *JINST* **3** (2008) S08004, doi:10.1088/1748-0221/3/08/S08004.

[23] J. Alwall et al., "MadGraph 5 : Going Beyond", *JHEP* **06** (2011) 128, doi:10.1007/JHEP06(2011)128, arXiv:1106.0522.

[24] NNPDF Collaboration, "Parton distributions for the LHC Run II", *JHEP* **04** (2015) 040, doi:10.1007/JHEP04(2015)040, arXiv:1410.8849.

[25] B. Fuks, M. Klasen, D. R. Lamprea, and M. Rothering, "Gaugino production in proton-proton collisions at a center-of-mass energy of 8 TeV", *JHEP* **1210** (2012) 081, doi:10.1007/JHEP10(2012)081, arXiv:1207.2159v2.

[26] B. Fuks, M. Klasen, D. R. Lamprea, and M. Rothering, "Precision predictions for electroweak superpartner production at hadron colliders with Resummino", *Eur. Phys. J. C* **73** (2013) 2480, doi:10.1140/epjc/s10052-013-2480-0, arXiv:1304.0790v2.

[27] P. Nason, "A New method for combining NLO QCD with shower Monte Carlo algorithms", *JHEP* **11** (2004) 040, doi:10.1088/1126-6708/2004/11/040, arXiv:hep-ph/0409146.

[28] S. Frixione, P. Nason, and C. Oleari, "Matching NLO QCD computations with Parton Shower simulations: the POWHEG method", *JHEP* **11** (2007) 070, doi:10.1088/1126-6708/2007/11/070, arXiv:0709.2092.

[29] Y. Gao et al., "Spin determination of single-produced resonances at hadron colliders", *Phys. Rev.* **D81** (2010) 075022, doi:10.1103/PhysRevD.81.075022, arXiv:1001.3396.

[30] S. Bolognesi et al., "On the spin and parity of a single-produced resonance at the LHC", *Phys. Rev.* **D86** (2012) 095031, doi:10.1103/PhysRevD.86.095031, arXiv:1208.4018.

[31] I. Anderson et al., "Constraining anomalous HVV interactions at proton and lepton colliders", *Phys. Rev.* **D89** (2014), no. 3, 035007, doi:10.1103/PhysRevD.89.035007, arXiv:1309.4819.

[32] A. V. Gritsan, R. Röntsch, M. Schulze, and M. Xiao, "Constraining anomalous Higgs boson couplings to the heavy flavor fermions using matrix element techniques", *Phys. Rev.* **D94** (2016), no. 5, 055023, doi:10.1103/PhysRevD.94.055023, arXiv:1606.03107.

[33] T. Sjöstrand, S. Mrenna, and P. Z. Skands, "PYTHIA 6.4 Physics and Manual", *JHEP* **05** (2006) 026, doi:10.1088/1126-6708/2006/05/026, arXiv:hep-ph/0603175.

[34] T. Sjöstrand et al., "An Introduction to PYTHIA 8.2", *Comput. Phys. Commun.* **191** (2015) 159–177, doi:10.1016/j.cpc.2015.01.024, arXiv:1410.3012.

[35] GEANT4 Collaboration, "GEANT4: A Simulation toolkit", *Nucl. Instrum. Meth.* **A506** (2003) 250–303, doi:10.1016/S0168-9002(03)01368-8.

[36] CMS Collaboration, "Particle-Flow Event Reconstruction in CMS and Performance for Jets, Taus, and MET", Technical Report CMS-PAS-PFT-09-001, CERN, Geneva, Apr, 2009.

[37] M. Cacciari, G. P. Salam, and G. Soyez, "The Anti-k(t) jet clustering algorithm", *JHEP* **04** (2008) 063, doi:10.1088/1126-6708/2008/04/063, arXiv:0802.1189.

[38] CMS Collaboration, "MET performance in 8 TeV data", Technical Report CMS-PAS-JME-12-002, CERN, Geneva, 2013.

[39] CMS Collaboration, "Measurement of the $t\bar{t}$ production cross section in the dilepton channel in pp collisions at $\sqrt{s} = 7$ TeV", *JHEP* **11** (2012) 067, doi:10.1007/JHEP11(2012)067, arXiv:1208.2671.

[40] T. Junk, "Confidence Level Computation for Combining Searches with Small Statistics", *Nucl. Instrum. Meth.* **A434** (1999) 435–443, doi:10.1016/S0168-9002(99)00498-2, arXiv:hep-ex/9902006.

[41] A. L. Read, "Modified frequentist analysis of search results (the CL_s method) in "Workshop on Confidence Limits", Eds. F. James, L. Lyons, and Y. Perrin",. p. 81.

[42] A. L. Read, "Presentation of search results: The CL(s) technique", *J. Phys. G* **28** (2002) 2693, doi:10.1088/0954-3899/28/10/313.

[43] ATLAS and CMS Collaborations, "Procedure for the LHC Higgs boson search combination in summer 2011", Technical Report CMS NOTE-2011/005, ATL-PHYS-PUB-2011-11, 2011.